U

UNSTABLE FLOW

T S Steenhuis, J-Y Parlange, and Y-J Kim, Cornell University, Ithaca, NY, USA
D A DiCarlo, USDA Agricultural Research Service, Oxford, MS, USA
J S Selker, Oregon State University, Corvallis, OR, USA
P A Nektarios, Agricultural University of Athens, Athens, Greece
D A Barry, University of Edinburgh, Edinburgh, UK
F Stagnitti, Deakin University, Warrnambool, VIC, Australia

Introduction

The importance of understanding unstable preferential flow processes cannot be overstated considering its relevance to crop irrigation, groundwater recharge, and vadose-zone transport of nutrients and contaminants. An important aspect of preferential infiltration is the residence time of water in the vadose zone, where contaminants and nutrients are degraded or exchanged in the media. The residence time is shorter for soils with preferential flow than without. Preferential flow can also be caused by macropores. Both types of preferential flow are similar in that the gravity force dominates sorptive processes. This article is concerned mainly with the unstable finger flow formation.

Conditions for Unstable Flow

Although the existence of fingered flow has been known since 1945, the practical importance of instability in stratified soils was not recognized prior to 1972, when Parlange and coworkers demonstrated that fingering can occur in a fine-over coarse-textured profile. In the early years, investigators were concerned with instabilities caused by gradients of temperature or solute concentration in miscible liquids. A few noticed that 'narrow tongues' formed in hydrophobic sands.

Several attempts were made in the 1950s and 1960s by Saffman and other researchers to relate the fingering in petroleum engineering to vadose-zone fingers; but this was problematic, because the first laboratory experiments used a viscous oil, glycerin, which was displaced by compressed air in Hele–Shaw cells. This is not an obvious analog to water displacing air in a stratified medium. As a consequence, viscosity became initially a dominant feature in many theories, although this is now known to be incorrect. This does not mean that some of the equations derived by Hele–Shaw cells cannot be properly reinterpreted. A necessary condition for instability, for water and air in a porous media, neglecting both viscosity and density of air, becomes:

$$K_s > Q \qquad [1]$$

where Q is the water flux imposed by the upper layer of fine material, and K_s is the saturated conductivity of water in the coarse layer underneath. The condition in eqn [1] is obviously necessary, because if Q was greater than K_s, the whole area would have to be saturated to carry the water and no finger would be present. It is a fundamental contribution of Hillel and coworkers to have noticed that eqn [1] is not constraining enough and that water entry in the coarse layer is associated with a 'water entry' suction for the water to penetrate the coarse layer. They further suggest that, upon rewetting, the water entry suction will be higher, resulting in drier fingers, leading to interesting hysteresis phenomena. In all cases, hysteresis is crucial by limiting lateral capillary diffusion of water which would otherwise remove the presence of fingers, as often happens in Hele–Shaw cells.

Finger Diameter and Structure

In early work in Hele–Shaw cells, the optimal width of the fingers was found by balancing the destabilizing effects of gravity and the stabilizing effect of surface tension. Finger width for soils were initially derived 'Green and Ampt soils,' with discontinuous wetting fronts. In the mid-1970s, Parlange and coworkers derived an expression for the finger

width, d, based on the analysis of Richards' equation, i.e., a diffuse front, yielding:

$$d = \pi \frac{S^2}{K(\theta - \theta_i)} \frac{1}{1 - Q/K} \quad [2]$$

where S is the sorptivity given by:

$$S_c^2 = \int_{\theta_i}^{\theta} D[\theta + \bar{\theta} - 2\theta_i] d\theta \quad [3]$$

where D is the soil-water diffusivity and θ_i is the initial water content, assumed small enough that the soil-water conductivity, K, at θ_i is negligible compared with its value at θ_c. The value of θ_c is a strong function of the initial water content and is not predicted by the theory. Equation [2] is valid for a two-dimensional finger in a slab chamber. In the field, where the fingers are three-dimensional π is replaced by 4.8.

Initially, for a soil initially dry, Parlange and coworkers assumed that θ_i in eqn [2] corresponds to saturation. However, fingers are rarely saturated in soils (as they are in a Hele–Shaw cells) and water content varies along the fingers. As shown in **Figure 1** the finger tip is the wettest (the red color) and it dries behind the finger. The moisture content, θ, varies with depth (measured from the interface between layers) according to the equation:

$$z = \int_{\theta_o}^{\theta} \frac{D d\bar{\theta}}{K - v(\bar{\theta} - \theta_i)} \quad [4]$$

where v is the constant downward speed of the fingers obtained after a short time, i.e., after all mergers have taken place and the fingers have reached a steady configuration. θ_o is the value of θ at $z = 0$ and, if we assume that the maximum value of θ corresponds to a water entry value θ_e, then eqn [4] gives:

$$vt = \int_{\theta_o}^{\theta_e} \frac{D d\theta}{K - v(\theta - \theta_i)} \quad [5]$$

which gives $\theta_o(t)$ when v and θ_e are known. In particular, when $t \to \infty$, θ_o approaches an asymptotic value $\theta_{o\infty}$ with:

$$K(\theta = \theta_{o\infty}) = v(\theta_{o\infty} - \theta_i) \quad [6]$$

When Q/K_c is negligible in eqn [2], we obtain a simpler equation for d:

$$d = \pi S_c^2 / K_c(\theta_c - \theta_i) \quad [7]$$

Note that both S_c^2 and K_c are inversely proportional to the viscosity; accordingly d is independent of viscosity. The influence of viscosity can be felt only through $[1 - Q/K_c]$ in eqn [2] and, thus, is irrelevant when fingering is important and Q/K_c is small.

Finally, for coarse sands, and as long as θ is not too small where the description of the Gardner–Ritsema soil-water conductivity is realistic:

$$K = K_c \exp \alpha(h - h_c) \quad [8]$$

where α is more or less constant and h is the matric potential. Then, eqn [3] shows that for a coarse sand:

$$S^2 \simeq 2(\theta - \theta_i) \frac{K_c}{\alpha} \quad [9]$$

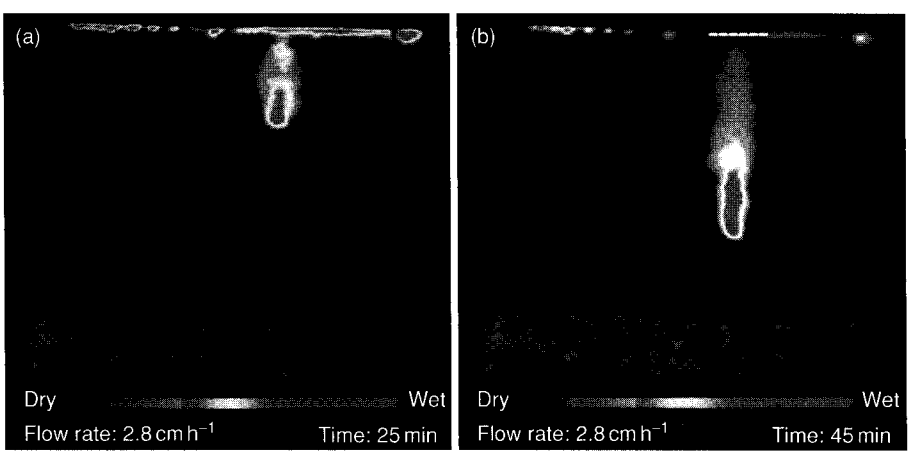

Figure 1 (see color plate 62) Finger formation in a coarse sand. Note that near the soil surface the distribution zone is visible. This zone carries the water from the rainfall that is uniformly applied at a rate of 2.8 cm h^{-1} to the one finger. Color indicates the moisture contents, with red the closest to saturation. Then the colors for decreasing moisture contents are: yellow, light green, light blue, dark blue, and black: (a) 25 min after water application; (b) 45 min after water application. Reproduced from Nektarios PA, Steenhuis TS, Petronic AM, and Parlange J-Y (1999) Fingered flow in laboratory golf putting greens. *Journal of Turfgrass Management* 3: 53–67.

Hence, we find the remarkably simple result:

$$d \simeq 2\pi/\alpha \qquad [10]$$

i.e., the dependence on θ_o and θ_i has disappeared. This explains why d is essentially constant in time and space and is inversely proportional to Gardner's α.

Note that, for water contents between θ_e and θ_o, all properties are measured on a drying curve of the matric potential. However, as the finger moves downwards within the sand, there is a very narrow zone at the finger tip where the water content increases rapidly, thus operating on a wetting curve, but reliable matric potential data are almost impossible to get in that region. Insight in this region was obtained by measuring reliable water contents down to the pore scale with neutron radiography. A 'dynamic' pressure, $h(\theta)$, was calculated based on Darcy's law by measuring the velocity of the finger, the distributed moisture content, and the unsaturated conductivity. The shape of the curve is similar to that which can be derived from earlier fingered flow experiments depicted in **Figure 2** and is very much different from expected soil-water pressure relationships for the same soil. Although these effects are sometimes attributed to nonequilibrium effects, applying continuum results to the pore scale is problematic.

In fingered flow experiments where initial moisture content is varied, the finger size initially decreases when the moisture content increases from 0 to 0.005 $cm^3\,cm^{-3}$ and then later increases with increasing moisture content when it reaches the width of the chamber at 0.04 $cm^3\,cm^{-3}$ (**Figure 3**; note that the

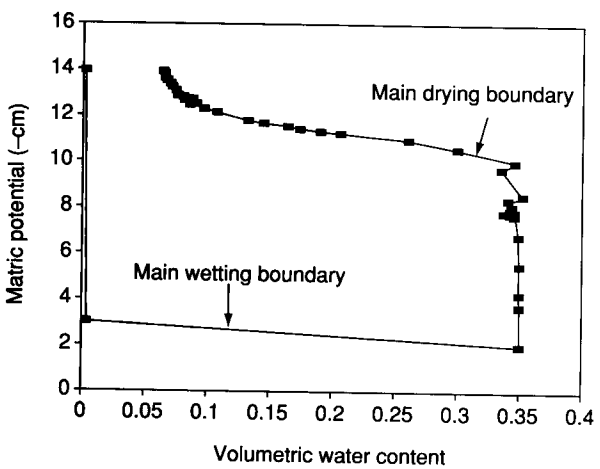

Figure 2 Nonequilibrium soil moisture curve obtained from fingered flow experiments. h, matric potential. Reproduced from Lin, Y, Steenhuis TS, and Parlange J-Y (1994) Closed-firm solution for finger width in sandy soils at different water contents. *Water Resource Research* 30: 951.

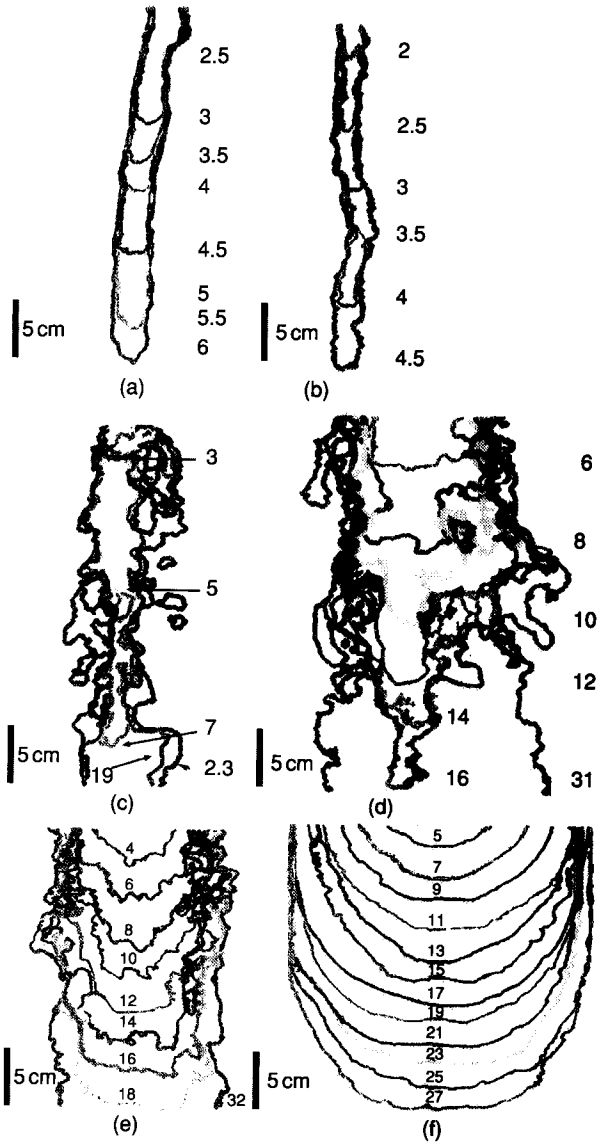

Figure 3 (a) Tracings of the totally dry sand. The sequence of tracings were taken every 30 s. The numbers accompanying the tracings are the minutes after infiltration started. A scale indicates 5 cm; (b) the advancing wetting front in the 0.01 $cm^3\,cm^{-3}$ moist sand. The infiltration front has a smaller width than in the totally dry case; (c) the advancing wetting front in the 0.02 $cm^3\,cm^{-3}$ initial moist sand pack. The tracings are depicted every 2 min. In addition, the latest tracing (after 23 min of infiltration) is shown; (d) advancing wetting fronts in the 0.03 $cm^3\,cm^{-3}$ moist sand. Two-minute tracings are shown until the front reached the bottom of the visible area. In addition, the tracing of the front is depicted when the infiltration was stopped (after 31 min); (e) advancing wetting fronts in the 0.04 $cm^3\,cm^{-3}$ initial moisture case. Two-minute tracings are shown until the front reached the bottom of the visible area. In addition, the front is depicted when the infiltration was stopped (after 32 min.); (f) the tracings of the wetting front when the chamber was imbibed from the bottom, or with a 0.04 $cm^3\,cm^{-3}$ (measured) initial moisture content. Tracings are depicted every 2 min. Reproduced with permission from Bauters TWJ, Dicarlo DA, Steenhuis TS, and Parlange J-Y (2000) Soil water content dependent wetting front characteristics in sands. *Journal of Hydrology* 231–232: 244–254.

surface induction zone is not shown). As θ_i increases, θ_c decreases rapidly and Q/K_c is not negligible in eqn [2] any more. Eqn [10] does not hold and d increases rapidly with θ_i.

The theory above applies only for a liquid, e.g., water or oil, and a gas, e.g., air. To extend the formula to the case of oil and water, it is necessary to obtain the dependence of the front velocity on its curvature. To obtain the dependence of the front velocity on curvature, the flow in the narrow diffuse region, ahead of it, must be analyzed, and to do so we must know the flow further ahead (here the pure oil). In the case of a gas, this presents no problem as it is assumed that the air can move freely ahead and does not affect the flow of water. Usually this will not be the case when oil is displaced by water, although it represents a limiting case.

The discussion has been limited, so far, to the movement of liquids. To include the transport of solutes, it is necessary to recall the physical configuration of the flow paths (**Figure 4**, where for clarity **Figure 1** has been redrawn schematically). The soil near the surface is more or less uniformly wet. This is the distribution zone in which water and solutes are funneled into the fingers of the conveyance zone below. The thickness of the distribution zone is that of the fine layer for layered soils and is of the order of the finger size for soils without such a layer. In the conveyance zone, all fingers move down with a velocity v. The number of fingers depends on the flow rate. For example, in **Figure 1** the flow rate is relatively low and only one finger is formed. In other experiments, where the flow rate is higher, several fingers form and, as a consequence, are spaced closer.

For the case when the initial concentration in the distribution zone is C_o, and the rainfall is solute-free, the concentration in the percolating water out of the

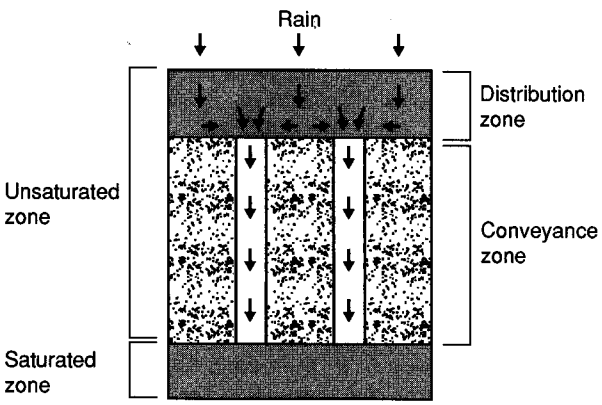

Figure 4 Schematic of the fingered flow process in the soil with preferential flow paths.

distribution zone can be described as similar to a linear reservoir:

$$C = C_o \exp(-\lambda t) \quad [11]$$

where λ is the coefficient equal to q/w, q is the steady-state flow rate, w is the apparent water content of the distribution zone and equals $L(\rho\, k_d + \theta_s)$, d is the depth of the distribution zone, θ_s is the saturated moisture content, ρ is the bulk density of the soil, and k_d is the desorption partition coefficient. In case water is added with a solute concentration, C_o, the concentration in the water leaving the distribution zone is:

$$C = C_o(1 - \exp(-\lambda t)) \quad [12]$$

Equations [11] and [12] are equivalent to those used for sludge by the US Environmental Protection Agency in predicting the loss of metals from the incorporation zone.

It is reasonable to assume that the transport in the preferential flow paths of the conveyance zone can be described with the convective–dispersive equation, viz:

$$D\frac{\partial^2 C}{\partial x^2} - v\frac{\partial C}{\partial x} = \frac{\partial C}{\partial t} \quad [13]$$

where D is the dispersion coefficient, and v is the velocity of the solute and equals approximately $q/(\beta(\rho\, k_d + \theta))$, where β is the wetted fraction in the conveyance zone by fingers and θ is the moisture content. Using Laplace transforms, eqn [13] can be integrated subject to the boundary condition described in eqn [11], with no solutes initially present in the column, and for $4D\,\lambda/v^2 < 1$ as:

$$C = \frac{1}{2}C_o \exp(-\lambda t)\left[\exp\left\{\frac{vx}{2D}(1-a)\right\}\operatorname{erfc}\left(\frac{x - vta}{2\sqrt{Dt}}\right) + \exp\left\{\frac{vx}{2D}(1+a)\right\}\operatorname{erfc}\left(\frac{x + vta}{2\sqrt{Dt}}\right)\right] \quad [14]$$

where

$$a = \sqrt{1 - \frac{4D\lambda}{v^2}}$$

The last term can usually be neglected when x or t is sufficiently large, i.e., $(x + vta)/(4Dt)_{1/2} > 3$. For the boundary condition (eqn [12]), we can find the solution by superposition.

Note that in eqn [14], as discussed above, the velocity is a function of the soil properties and not of the flow rate. The number of fingers in the conveyance zone adjusts itself to facilitate the different flow rates. This has been demonstrated with a fingered

flow experiment that was carried out in the laboratory with 50-cm-long, 14-cm-diameter duplicate columns filled with coarse sand subjected to different intensities of steady-state rainfall. Chloride was applied at the surface as a pulse during each steady-state rainfall using different columns for different flow rates. The results are given as a function of cumulative flow (**Figure 5a**) rate and time (**Figure 5b**). In **Figure 5a**, the initial breakthrough of chloride takes more water for the high flow rate of 2 cm h^{-1} than for the low flow rate (0.3 cm h^{-1}). This is, obviously, a direct consequence of having a greater portion of the column wetted for the high flow rate. In **Figure 5b**, when chloride concentrations are plotted as a function of time, initial breakthrough for all three flow rates is approximately at the same time, clearly establishing that water and solute velocity is the same for the different flow rates. When the results are fitted to eqn [14], the solute velocity is, in all cases, approximately 35 cm h^{-1}, with no clear trend among the different flow rates, as expected.

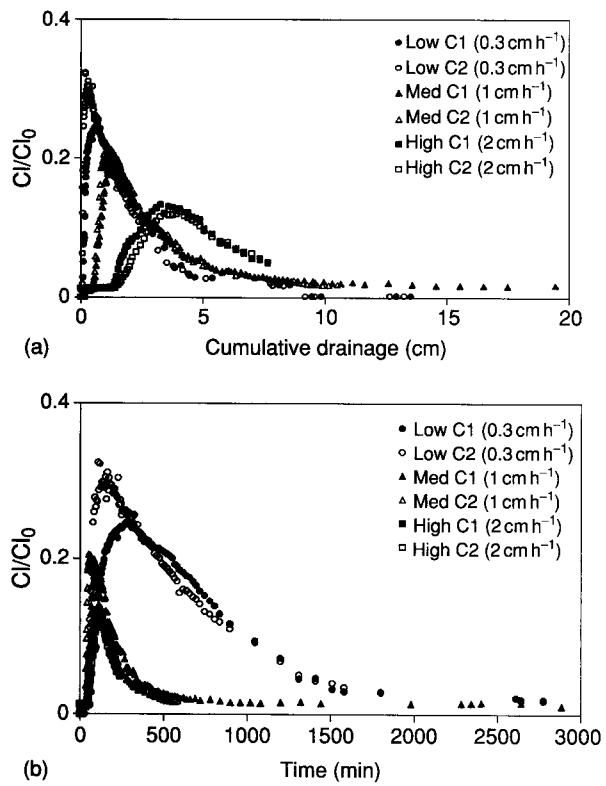

Figure 5 Chloride breakthrough curves (CBTs) for sand columns with a pulse application for three different flow rates of 0.3, 1, and 2 cm h^{-1} plotted: (a) as a function of cumulative drainage after application of the chloride pulse; (b) as a function of time after application of the chloride pulse. The experiment was carried out in duplicate with C1 and C2 indicating the two columns.

In conclusion, it has become obvious in the last 25 years that, for soils in the field, preferential flow is the rule rather than the exception. Fingered flow is one of these types of preferential flow and can often be found above the primary coastal aquifers that are overlain by coarse-grained soils. Recognizing that these fingered flow paths can rapidly carry chemicals down to groundwater is a first step in keeping our aquifers clean for generations to come.

Further Reading

Bauters TWJ, DiCarlo DA, Steenhuis TS, and Parlange J-Y (2000) Soil water content dependent wetting front characteristics in sands. *Journal of Hydrology* 231–232: 244–254.

DeBano LF and Dekker LW (2000) Water repellency bibliography. *Journal of Hydrology* 231–232: 409–432.

Glass RJ, Steenhuis TS, and Parlange J-Y (1989) Mechanism for finger persistence in homogeneous, unsaturated, porous media: theory and verification. *Soil Science* 148: 60–70.

Hill DE and Parlange J-Y (1972) Wetting front instability in homogeneous soils. *Soil Science Society of America Proceedings* 36: 697–702.

Hillel D (1987) Unstable flow in layered soils: a review. *Hydrological Processes* 1: 143–147.

Parlange J-Y and Hill DE (1976) Theoretical analysis of wetting front instability in soils. *Soil Science* 122: 236–239.

Philip JR (1975) Stability analysis of infiltration. *Soil Science Society of America Proceedings* 39: 1042–1049.

Raats PAC (1973) Unstable wetting fronts in uniform and nonuniform soils. *Soil Science Society of America Proceedings* 37: 681–685.

Saffman PG and Taylor GI (1958) The penetration of a fluid into a porous medium or Hele-Shaw cell containing a more viscous liquid. *Proceedings of the Royal Society of London. Series A: Mathematical and Physical Sciences* 245: 312–331.

Selker J, Leclerq P, Parlange J-Y, and Steenhuis TS (1992a) Fingered flow in two dimensions. 1. Measurement of matric potential. *Water Resources Research* 28: 2513–2521.

Selker J, Parlange J-Y, and Steenhuis TS (1992b) Fingered flow in two dimensions. 2. Predicting finger moisture profile. *Water Resources Research* 28: 2523–2528.

Steenhuis TS, Boll J, Shalit G, and Merwin IA (1994) A simple equation for predicting preferential flow solute concentration. *Journal of Environmental Quality* 23: 1058–1064.